Sustainable Cities and Society 35 (2017) 841–850

Contents lists available at ScienceDirect

Sustainable Cities and Society

journal homepage: www.elsevier.com/locate/scs

Characterization of different heat mitigation strategies in landscape to fight against heat island and improve thermal comfort in hot-humid climate (Part II): Evaluation and characterization

T.F. Zhao[a], K.F. Fong[b,*]

[a] Department of Architecture and Civil Engineering, College of Science and Engineering, City University of Hong Kong, Hong Kong, China
[b] Division of Building Science and Technology, College of Science and Engineering, City University of Hong Kong, Hong Kong, China

ARTICLE INFO

Keywords:
Heat mitigation strategy
Urban heat island
Outdoor thermal comfort
Landscape design
Urban open space model
Hot and humid climate

ABSTRACT

This is Part II of the study, aiming at analyzing and characterizing the cooling potentials of heat mitigation strategy (HMS) in landscape from both combating urban heat island (UHI) and alleviating human heat stress, in terms of air temperature reduction ΔT_a and Physiological Equivalent Temperature reduction ΔPET respectively. Here, different HMSs for landscape design were investigated, including vegetation (Green-HMS), high albedo pavement (Grey-HMS), water body (Blue-HMS) and hybrid of trees and landscaping surface (Hybrid-HMS). Parametric study was conducted with a validated urban open space model developed from ENVI-met V4. Through ΔT_a and ΔPET, the cooling benefits of each HMS were evaluated with the area coverage ratio R_{HMS} and the corresponding parameters. Generally, larger R_{MHS} would have both higher ΔT_a and ΔPET in various HMSs, except Grey-HMS. Hybrid-HMS demonstrates the greatest heat mitigation potentials, followed by Green-HMS, Blue-HMS and Grey-HMS. Hybrid-HMS has further cooling benefits compared to the landscape design with singular HMS. For Grey-HMS or Blue-HMS, its heat mitigation potential evaluated by ΔT_a is different from that by ΔPET, so both aspects should be considered in landscape design. Consequently, characterization charts of different HMSs are established, which would help the urban design practitioners create comfortable open spaces in hot-humid climate.

1. Introduction

As cities around the world continue to urbanize, there is an increasing body of evidence suggesting that urbanization has led to the 'urban heat island (UHI)' phenomenon (Cui & Shi, 2012; Santamouris, 2007), whereby cities become warmer than the surrounding suburbs. In other words, there is a temperature difference between cities and the areas surrounding them (Oke, 1982). Deteriorating thermal environment in cities represents a great challenge to fight against UHI and improve thermal comfort by sustainable urban design. Heat mitigation is therefore necessary. Jackson (1985) defined urban open spaces as an urban form that draws people together for passive enjoyment. The links between urban open spaces and environmental quality were outlined by Rogers (1999). Proper landscape design of urban open spaces helps improve the thermal environment and encourage people's outdoor activities. Vegetation, high albedo and water body have been acknowledged as effective heat mitigation strategy (HMS) in landscape design. Quantifying the associated heat mitigation potential is crucial for effective design guidance. However, current studies in this area are far from sufficiency. Hence, this study primarily focuses on characterizing the cooling potentials of various heat mitigation strategies (HMSs) in landscape from both combating UHI and alleviating human heat stress. In Part I of this study, thermal performance of different HMSs in landscape of real urban environment was investigated by field measurement. It was found that the variations in air temperature and mean radiant temperature could reach 4.5 °C and 32 °C respectively, which was substantial in landscape of a campus scale. The existence of local heat island, as well as the relationship between microclimate and HMSs, was verified. A landscape model was developed with the microclimate simulation tool ENVI-met and validated by the field measurement data. As Part II of this study, the developed model has been carried forward here for ongoing evaluation and characterization of different HMSs in landscape.

2. Methodology

Based on the validated simulation settings in Part I of this study, a new model was built for conducting the parametric study of various test

* Corresponding author at: 8 Tat Chee Avenue, Kowloon Tong, Hong Kong, China.
E-mail address: bssquare@cityu.edu.hk (K.F. Fong).

http://dx.doi.org/10.1016/j.scs.2017.05.006

Available online 05 May 2017
2210-6707/

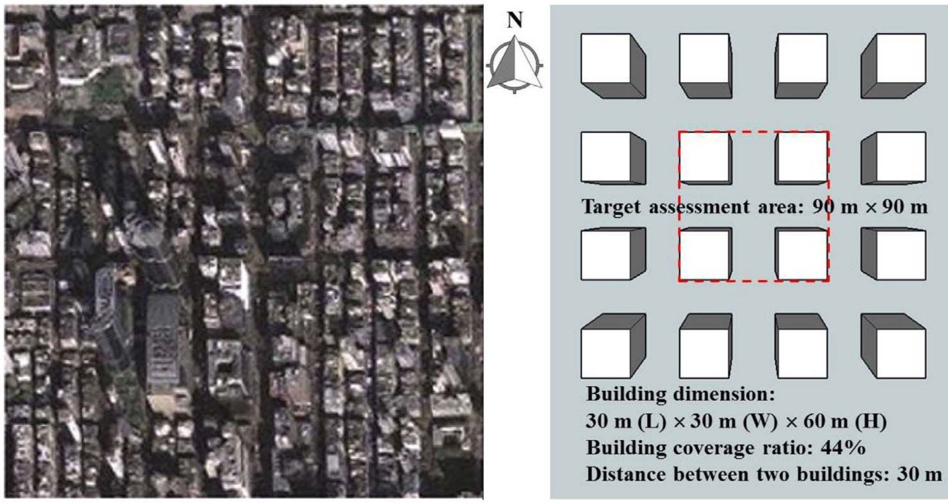

Fig. 1. Typical urban morphology in Hong Kong (left) and the associated urban open space model (right).

cases of HMSs. As such, an urban open space model was established based on the typical urban morphology in Hong Kong, as shown in Fig. 1. The building coverage ratio of the target assessment area was 44%, which is the average value in Hong Kong (Ng, Chen, Wang, & Yuan, 2012). HMS was implemented in the open space remained, accounting for 56% of the target assessment area. Similar generic urban building block models were used in the previous studies (Jackson, 1985; Yuminoa, Uchidaa, Sasaki, Kobayashi, & Mochidaa, 2015). To include the effect of the surrounding buildings in a real life situation, buildings with similar dimensions were added around the target assessment area.

From Fig. 1, the open space was in a “cross” shape as formed by five squares. In each test case, 9 receptor points were evenly distributed in each square of the open space, altogether 45 sets of T_a and *PET* results from the receptor points could be used for analysis. This had the advantage of giving a complete spatial survey of the local microclimate conditions compared to single point investigation. Fig. 2 shows the distribution of receptor points in the open space model. Table 1 consolidates all the cases in the parametric study according to the following category of landscape designs:

- Base case: Conventional landscape with concrete pavement;
- Green-HMS: Implementation of vegetation with varying area coverage ratios, vegetation types and tree canopy densities;
- Grey-HMS: Implementation of high albedo pavement with varying area coverage ratios and albedo values;
- Blue-HMS: Implementation of water body with varying area coverage ratios; and
- Hybrid-HMS: Implementation of combination of high-canopy-density trees and particular ground surface material with varying area coverage ratios.

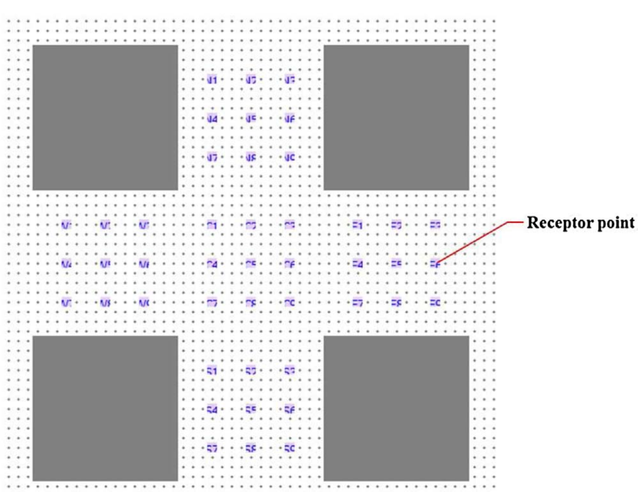

Fig. 2. Distribution of receptor points in the open space model.

The albedo of main ground surface materials and trees are listed in Table 2. The distribution of HMSs in different cases under varying area coverage ratio (from 8% to 56%) is shown in Fig. 3.

3. Results and discussion

As mentioned before, the cooling benefits should not be only evaluated by combating heat island in term of T_a, but also the thermal comfort conditions of pedestrians in terms of *PET* in urban open space. The heat mitigation potentials based on T_a and *PET* were primarily evaluated with R_{HMS} of 56%, 34%, 16%, 8% for Green-HMS, Grey-HMS, Blue-HMS and Hybrid-HMS, as well as 0% for the conventional landscape design. The effects of other design parameters were also assessed in the corresponding HMSs when necessary. All simulation results referred to a height of 1.5 m above ground. Here, the mid-afternoon microclimate was focused on since it would have the maximum thermal stress on pedestrians, and the simulation results of 15:00 were then used.

3.1. Effect of landscape design on average T_a and PET

Table 3 summarizes the average T_a and *PET* at a height of 1.5 m for all the cases at 15:00. For the conventional landscape with 0% R_{HMS} (i.e. 56% concrete pavement), the average T_a was high at 34.8 °C, indicating high heat stress in the urban open space. With respect to *PET*, the average value was 48.2 °C, which was significantly higher than 28.1 °C, the neutral *PET* in summer as found in an outdoor thermal comfort study for Hong Kong (Ng & Cheng, 2012). As such, the conventional landscape would create an uncomfortable thermal environment for pedestrians in the urban outdoor open space.

For every case of HMS, it is found that the average T_a was increased with the drop of R_{HMS} as shown in Table 3. In other words, higher R_{HMS} would enhance the reduction of T_a. The average *PET* had a similar trend in general. But for Grey-HMS (i.e. Cases A1 to A4), the average *PET* was decreased with R_{HMS}. Compared to the base case, all HMSs demonstrated clear cooling potentials in lowering T_a and *PET*, except that Grey-HMS had cooling benefit in T_a only. The average *PET* of Grey-HMS were all higher than that of the conventional case, making the thermal

Table 1
Summary of the configurations of various cases of landscape designs.

Case	Landscape design	Case code	Area coverage ratio of HMS R_{HMS}	Area coverage ratio of conventional hard surface
Conventional landscape (Base case)	Concrete pavement	C	0%	56%
Green-HMS	Grass	G_1	56%	0%
		G_2	34%	22%
		G_3	16%	40%
		G_4	8%	48%
	High-canopy-density trees + Concrete pavement (LAI = 9.35)	$[T_HC]_1$	56%	0%
		$[T_HC]_2$	34%	22%
		$[T_HC]_3$	16%	40%
		$[T_HC]_4$	8%	48%
	Medium-canopy-density trees + Concrete pavement (LAI = 3.65)	$[T_MC]_1$	56%	0%
		$[T_MC]_2$	34%	22%
		$[T_MC]_3$	16%	40%
		$[T_MC]_4$	8%	48%
	Low-canopy-density trees + Concrete pavement (LAI = 0.93)	$[T_LC]_1$	56%	0%
		$[T_LC]_2$	34%	22%
		$[T_LC]_3$	16%	40%
		$[T_LC]_4$	8%	48%
Grey-HMS	High albedo pavement (α = 0.6)	$[A1]_1$	56%	0%
		$[A1]_2$	34%	22%
		$[A1]_3$	16%	40%
		$[A1]_4$	8%	48%
	High albedo pavement (α = 0.7)	$[A2]_1$	56%	0%
		$[A2]_2$	34%	22%
		$[A2]_3$	16%	40%
		$[A2]_4$	8%	48%
	High albedo pavement (α = 0.8)	$[A3]_1$	56%	0%
		$[A3]_2$	34%	22%
		$[A3]_3$	16%	40%
		$[A3]_4$	8%	48%
	High albedo pavement (α = 0.9)	$[A4]_1$	56%	0%
		$[A4]_2$	34%	22%
		$[A4]_3$	16%	40%
		$[A4]_4$	8%	48%
Blue-HMS	Water body	W_1	56%	0%
		W_2	34%	22%
		W_3	16%	40%
		W_4	8%	48%
Hybrid-HMS	High-canopy-density trees + Concrete pavement (identical to that of Green-HMS)	$[T_HC]_1$	56%	0%
		$[T_HC]_2$	34%	22%
		$[T_HC]_3$	16%	40%
		$[T_HC]_4$	8%	48%
	High-canopy-density trees + High albedo pavement (α = 0.9)	$[T_HA]_1$	56%	0%
		$[T_HA]_2$	34%	22%
		$[T_HA]_3$	16%	40%
		$[T_HA]_4$	8%	48%
	High-canopy-density trees + Soil	$[T_HS]_1$	56%	0%
		$[T_HS]_2$	34%	22%
		$[T_HS]_3$	16%	40%
		$[T_HS]_4$	8%	48%
	High-canopy-density trees + Grass	$[T_HG]_1$	56%	0%
		$[T_HG]_2$	34%	22%
		$[T_HG]_3$	16%	40%
		$[T_HG]_4$	8%	48%

comfort problem worse.

3.2. Analysis of quartile distributions of T_a and *PET*

To understand more clearly about the cooling potentials of the various HMSs, the quartile distributions of both T_a and *PET* were analysed. In the following figures related to quartile distributions, the information of maximum, median, minimum and range of each quartile are presented. In addition, the average value from Table 3 is also marked on the corresponding interquartile range with a small square box for each case.

Table 2
The albedo (α) of main ground surface materials and trees.

Ground surface materials/trees	α
Concrete pavement	0.2
Grass	0.2
Trees	0.2
High albedo pavement	0.6/0.7/0.8/0.9
Soil	0.0

3.2.1. Green-HMS

Fig. 4 depicts the quartile distribution of T_a and *PET* of Green-HMS. The horizontal dotted line represents the average T_a (34.8 °C) and the average *PET* (48.2 °C) of the base case at 15:00. The average T_a of the base case was higher than the maximum T_a of every case investigated, indicating that there was definite cooling potential of T_a in all the Green-HMS. In general, the average *PET* of the base case was higher than the interquartile ranges involved, but it could not fully bound the first quartiles of Case G at 34% R_{HMS}, Cases G and T_LC at 16% R_{HMS}, and all the cases at 8% R_{HMS}. Nevertheless, this shows that Green-HMS could generally improve thermal comfort in the open space, in particular when R_{HMS} was above 34%.

It is found that both the interquartile ranges of T_a and *PET* are getting widened with the decline of R_{HMS} for each case of Green-HMS in Fig. 4. This indicates larger spatial variations of T_a and *PET*, resulting more uneven thermal environment in the open space at smaller R_{HMS}. For the *PET* distributions among all the cases of Green-HMS, those of Cases G were the widest, showing that the spatial variation of thermal comfort was the largest. Compared to the cases with trees, grass itself had the least capacity to mitigate the thermal environment for human comfort.

In Fig. 4, the rising trends of the average T_a and *PET* for the cases with trees (i.e. T_HC, T_MC and T_LC) illustrate that the tree canopy density, as governed by LAI, is another significant parameter of heat mitigation potential. High-canopy-density trees showed the highest cooling potential in terms of T_a and *PET*, followed by medium- and low-canopy-density trees. This is because higher LAI values are correlated to larger magnitude of solar attenuation. In other words, trees with higher canopy density would produce lower amount of radiant heat underneath, resulting in less terrestrial radiation, hence lower T_{mrt} in the landscape and surrounding area. In fact, T_{mrt} is the most important factor in determining thermal comfort (Ali-Toudert, 2005).

Type of vegetation (i.e. grass or tree) is another parameter of cooling potential as observed from Fig. 4. Grass showed stronger heat mitigation potential than medium- and low-canopy-density trees in view of the average T_a. Even though trees can create shades, certain amount of radiation is still absorbed by the concrete ground surfaces, which increases the surrounding thermal condition. However, grass would contribute and lower the surface temperature, thus it is possible to obtain lower ambient air temperature by convection. As previously mentioned, grass has the least cooling benefit in the aspect of *PET*, since it is unlike the medium- and low-canopy-density trees to reduce the radiative flux.

3.2.2. Grey-HMS and Blue-HMS

Fig. 5 illustrates the quartile distributions of T_a and *PET* of Grey-HMS and Blue-HMS. The dotted line for the mean T_a of the base case is located above the maximum T_a of all the cases investigated. It reveals

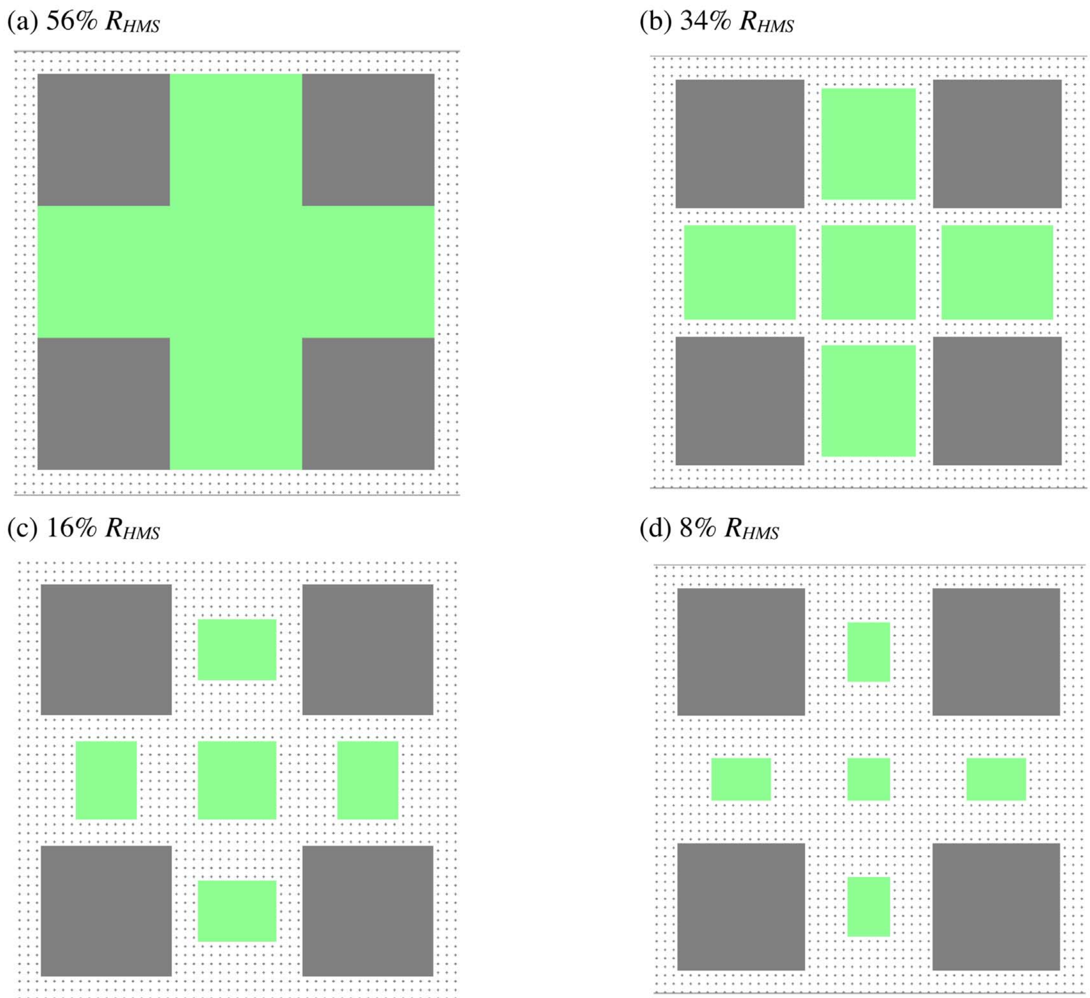

Fig. 3. HMSs in different cases under varying area coverage ratio.

that implementation of Grey-HMS and Blue-HMS are effective in combating UHI in landscape. In Fig. 5(a), the interquartile ranges of T_a for every case in Grey-HMS/Blue-HMS are steadily widened when R_{HMS} is reduced, suggesting the variance is getting high in the thermal environment.

For Grey-HMS, the albedo values of surface materials would affect the heat mitigation potential. By absorbing less incident solar radiation, higher albedo value of pavements would gain more cooling benefit in terms of T_a. Simultaneously, less long-wave heat is released back to the surrounding thus T_a can be lower. Blue-HMS has a different cooling mechanism. Evaporation of water from water body would cool its surface, and high heat capacity of water makes it not heated up as quickly as the concrete surface. As a result, Blue-HMS can have the lowest interquartile range at each R_{HMS} as shown in Fig. 5(a).

Table 3
Average T_a and *PET* at a height of 1.5 m for different R_{HMS} in various cases at 15:00.

Case	Average T_a (°C)					Average *PET* (°C)				
	56% (1)	34% (2)	16% (3)	8% (4)	0%	56% (1)	34% (2)	16% (3)	8% (4)	0%
Conventional	–	–	–	–	34.8	–	–	–	–	48.2
G	32.8	33.0	33.2	33.4	–	43.5	43.8	44.1	44.4	–
T_HC	32.6	32.9	33.2	33.4	–	36.8	37.5	39.8	43.0	–
T_MC	33.0	33.2	33.3	33.4	–	37.9	38.8	40.5	43.4	–
T_LC	33.4	33.4	33.4	33.5	–	41.2	41.6	42.5	44.1	–
A1	33.8	34.0	34.2	34.3	–	49.8	49.6	49.5	49.4	–
A2	33.7	33.9	34.2	34.3	–	49.9	49.7	49.5	49.4	–
A3	33.6	33.8	34.1	34.2	–	49.9	49.7	49.6	49.4	–
A4	33.4	33.8	34.1	34.2	–	50	49.7	49.6	49.4	–
W	33.3	33.6	34.0	34.1	–	47.5	48.2	48.8	49.0	–
T_HA	32.5	32.8	33.1	33.3	–	36.7	37.5	39.8	43.1	–
T_HS	32.2	32.7	33.1	33.3	–	36.3	37.2	39.6	43.0	–
T_HG	31.9	32.5	32.9	33.2	–	35.8	36.5	39.1	42.5	–

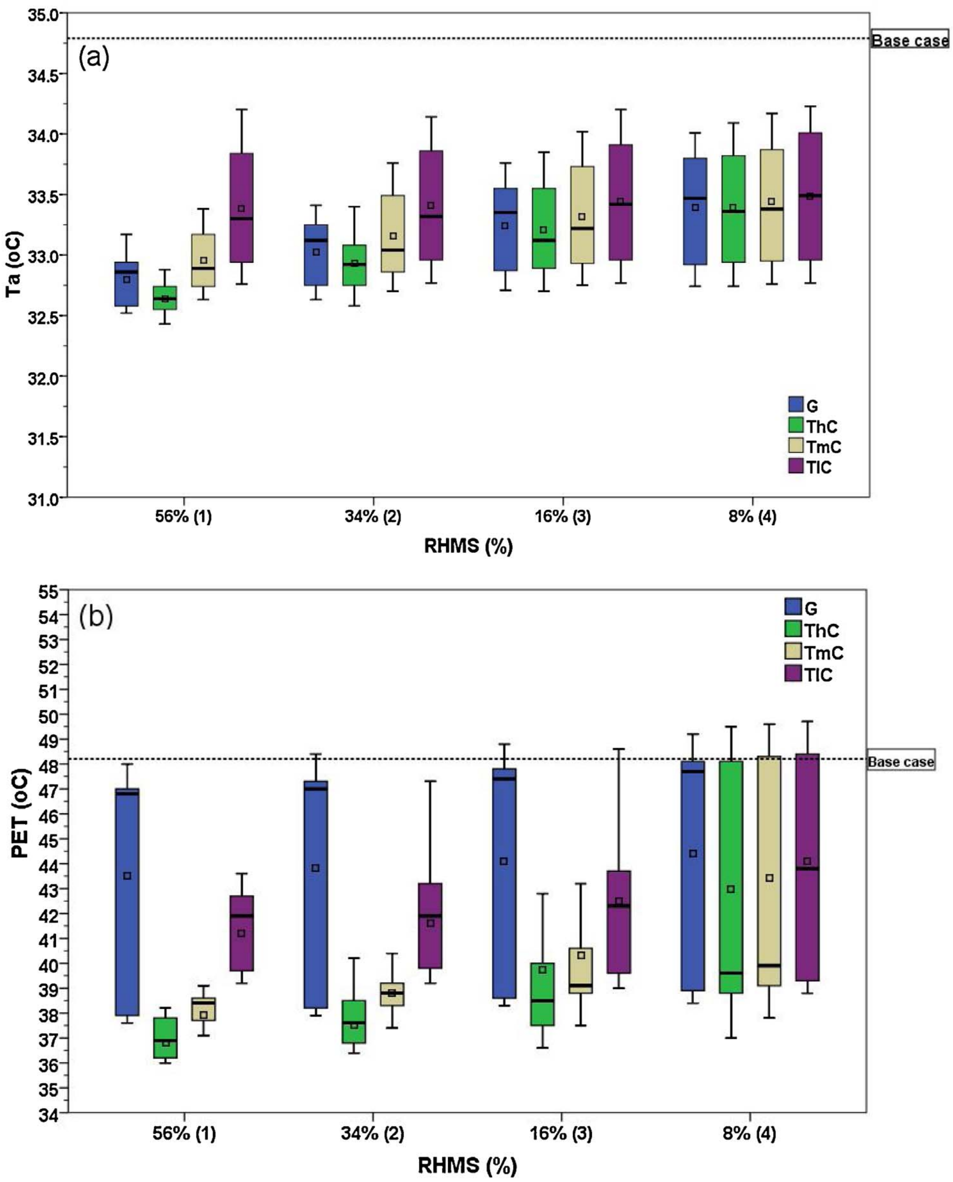

Fig. 4. Quartile distributions of T_a (a) and *PET* (b) at 15:00 for different cases of Green-HMS.

In Fig. 5(b), most *PET* values of the cases distributed above the average *PET* of the base case. Grey-HMS was found with negative effect on thermal comfort, although it could effectively fight against heat island. The greater the albedo value, the higher *PET* was. Despite lower T_a could be obtained by Grey-HMS, large amount of radiative flux, especially short-wave radiation, is reflected back towards all directions, including the pedestrian level. It largely increases T_{mrt}, thus aggravating the thermal comfort conditions. On the other hand, Blue-HMS would demonstrate the possibility to improve thermal comfort, but R_{HMS} should be above 34% so that the average *PET* could be higher than that of the base case. This is because *PET* was mainly determined by the integral effect of T_a, *RH* and T_{mrt}. The cooling effect of water body due to its evaporation, high heat capacity and high emissivity would favor the reduction of both T_a and T_{mrt}. However, the increase of *RH* through water evaporation would decrease heat loss from human body and exert negative influence on thermal comfort (ASCE, 2004; Stathopoulos, 2006). When R_{HMS} is up to a certain level, the combined cooling merit of T_a and T_{mrt} would outweigh the disadvantage of *RH*. Therefore, as found in this study, it is necessary to have large enough water surface area in order to remedy the human thermal stress. From Fig. 5(b), it is also observed that the interquartile ranges of *PET* for Grey-HMS/Blue-HMS remained large without much difference in varying R_{HMS}, showing that large spatial variation of thermal comfort existed in the open space.

3.2.3. Hybrid-HMS

Fig. 6 depicts the quartile distributions of T_a and *PET* of Hybrid-HMS. It demonstrates further cooling potential on top of T_HC, a singular heat mitigation case of Green-HMS. Compared to the base case, the interquartile ranges of T_a and most of *PET* are under the respective dotted lines. This indicates that the cooling effects of Hybrid-HMS would be enhanced when the already reduced amount of incoming solar radiation on the ground can be further controlled by the ground surface material underneath the tree canopy. Actually Hybrid-HMS could intercept much solar radiation and reduce the absorption of radiation of ground surface, hence lower the surface and surrounding air temperatures. As a result, both T_a and *PET* can be effectively reduced in the urban open space.

Among the various Hybrid-HMS, the greatest cooling benefits could be obtained from the case T_HG, in which the concrete ground surface of trees was changed to grass, followed by T_HS with soil surface, then T_HA with high albedo pavement, and T_HC with concrete surface the least. This is closely related to the cooling capacity of ground surfaces under

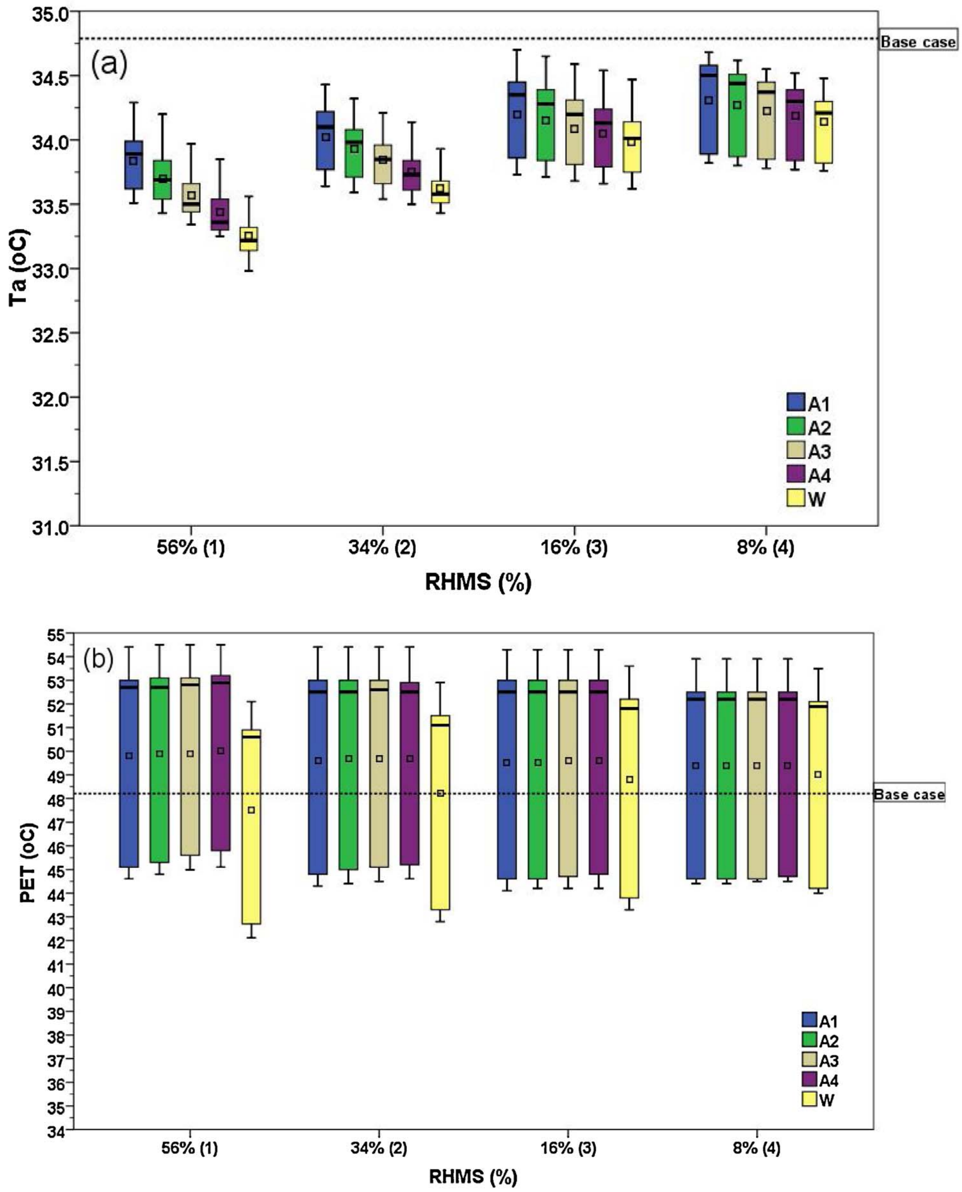

Fig. 5. Quartile distributions of T_a (a) and *PET* (b) at 15:00 for different cases of Grey-HMS and Blue-HMS.

the tree. Via shading and evapotranspiration, the grassland could maintain the lowest surface temperature. Soil is a natural heat sink, and large heat capacity makes it not easy to be heated up. For high albedo pavement, its reflection capacity of solar radiation contributes a lower surface temperature, but probably a higher T_{mrt}. As R_{HMS} decreased, both the interquartile ranges of T_a and *PET* were enlarged. In Fig. 6(b), the ranges of *PET* of the various Hybrid-HMS remained relatively stable when R_{HMS} was 16% and above, which suggested their good ability in maintaining thermal comfort of open space.

3.3. Characterization of heat mitigation potential of different HMS

3.3.1. Evaluation of heat mitigation potentials through T_a and *PET* reductions

Besides looking at the absolute values of the averages and the quartile distributions of T_a and *PET*, it would be more effective to interpret the cooling potentials of various heat mitigation strategies by using the difference between the data of HMS and that of the base case from Table 3. As such, Table 4 was generated to present the T_a reduction, ΔT_a, and the *PET* reduction, ΔPET, for R_{HMS} increased from 8% to 56%.

For Green-HMS, with gradually increased R_{HMS} from 8% to 56%, ΔT_a was raised in the ranges of 1.4–2.0 °C, 1.4–2.2 °C, 1.4–1.8 °C, and 1.3–1.4 °C for Cases G, T_HC, T_MC and T_LC, respectively. The corresponding ΔPET ranges were 3.8–4.7 °C, 5.2–11.4 °C, 4.8–10.3 °C, and 4.1–7.0 °C. It proves that Green-HMS has good ability in combating heat island and improving thermal comfort. In addition, differences in ΔT_a and ΔPET could reach up to 0.8 °C and 6.7 °C respectively among the cases of Green-HMS at 56% R_{HMS}.

Grey-HMS could have the corresponding ΔT_a ranges of 0.5–1.0 °C, 0.5–1.1 °C, 0.6–1.2 °C and 0.6–1.4 °C for Cases A1–A4, respectively. The difference in ΔT_a among different cases of albedos could be up to 0.4 °C at 56% R_{HMS}. However, Grey-HMS had the problem of negative ΔPET in all cases, with Case A4 the worst at −1.8 °C. As discussed before, Grey-HMS is tangible in fighting UHI but not capable to facilitate thermal comfort. For Blue-HMS, ΔT_a would be 0.7–1.5 °C for 8–56% R_{HMS}. ΔPET would turn from negative to positive in case R_{HMS} was greater than 34%, and it could be up to 0.7 °C. With sufficiently large R_{HMS}, Blue-HMS is still an effective mean in both combating heat island and improving thermal comfort.

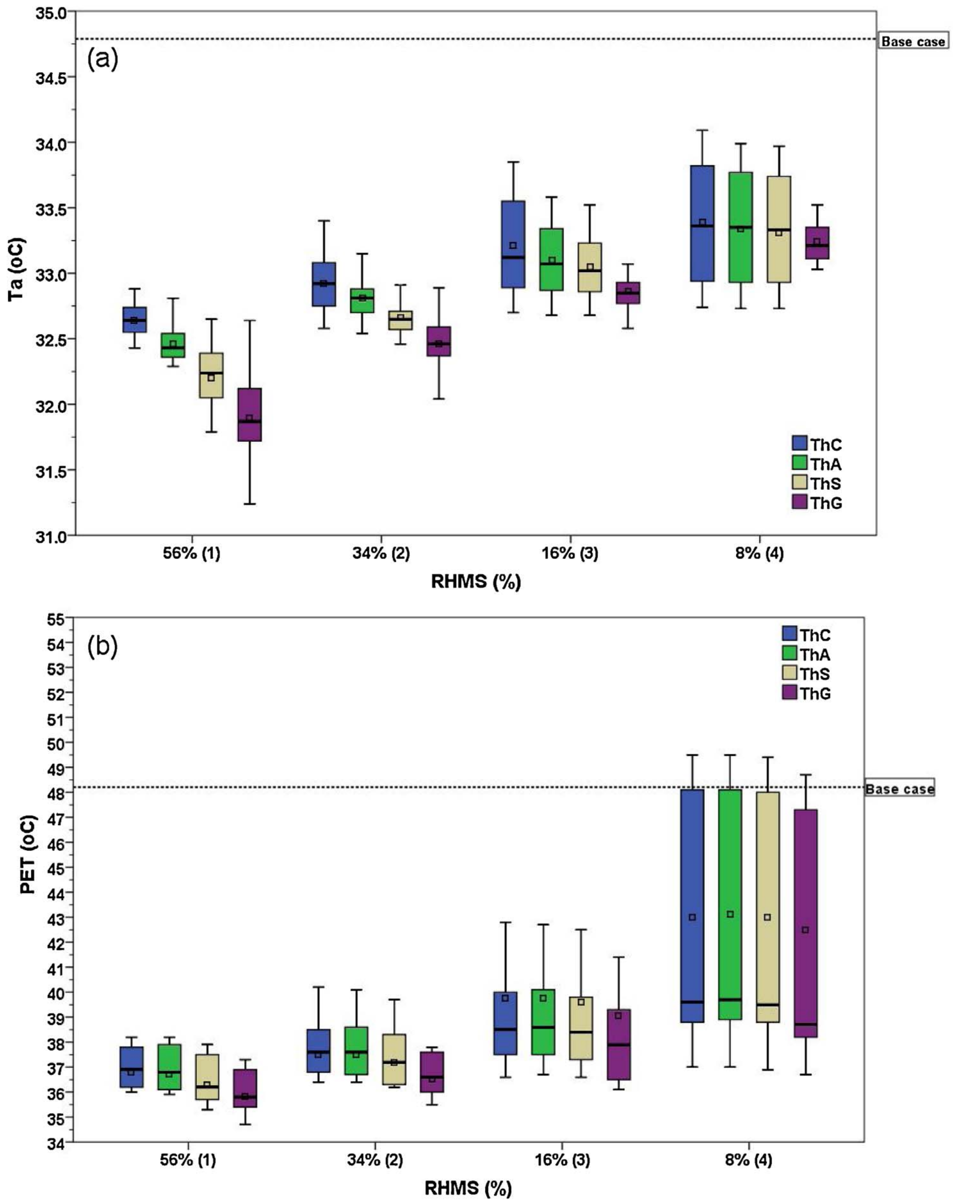

Fig. 6. Quartile distributions of T_a (a) and *PET* (b) at 15:00 for different cases of Hybrid-HMS.

Table 4
ΔT_a and ΔPET at a height of 1.5 m for different R_{HMS} in various cases at 15:00.

Case	ΔT_a (°C)				ΔPET (°C)			
	4 (8%)	3 (16%)	2 (34%)	1 (56%)	4 (8%)	3 (16%)	2 (34%)	1 (56%)
G	1.4	1.6	1.8	2.0	3.8	4.1	4.4	4.7
T_HC	1.4	1.6	1.9	2.2	5.2	8.4	10.7	11.4
T_MC	1.4	1.5	1.6	1.8	4.8	7.7	9.4	10.3
T_LC	1.3	1.4	1.4	1.4	4.1	5.7	6.6	7.0
A1	0.5	0.6	0.8	1.0	−1.2	−1.3	−1.4	−1.6
A2	0.5	0.6	0.9	1.1	−1.2	−1.3	−1.5	−1.7
A3	0.6	0.7	1.0	1.2	−1.2	−1.4	−1.5	−1.7
A4	0.6	0.7	1.0	1.4	−1.2	−1.4	−1.5	−1.8
W	0.7	0.8	1.2	1.5	−0.8	−0.6	0	0.7
T_HA	1.5	1.7	2.0	2.3	5.1	8.4	10.7	11.5
T_HS	1.5	1.7	2.1	2.6	5.2	8.6	11.0	11.9
T_HG	1.6	1.9	2.3	2.9	5.7	9.1	11.7	12.4

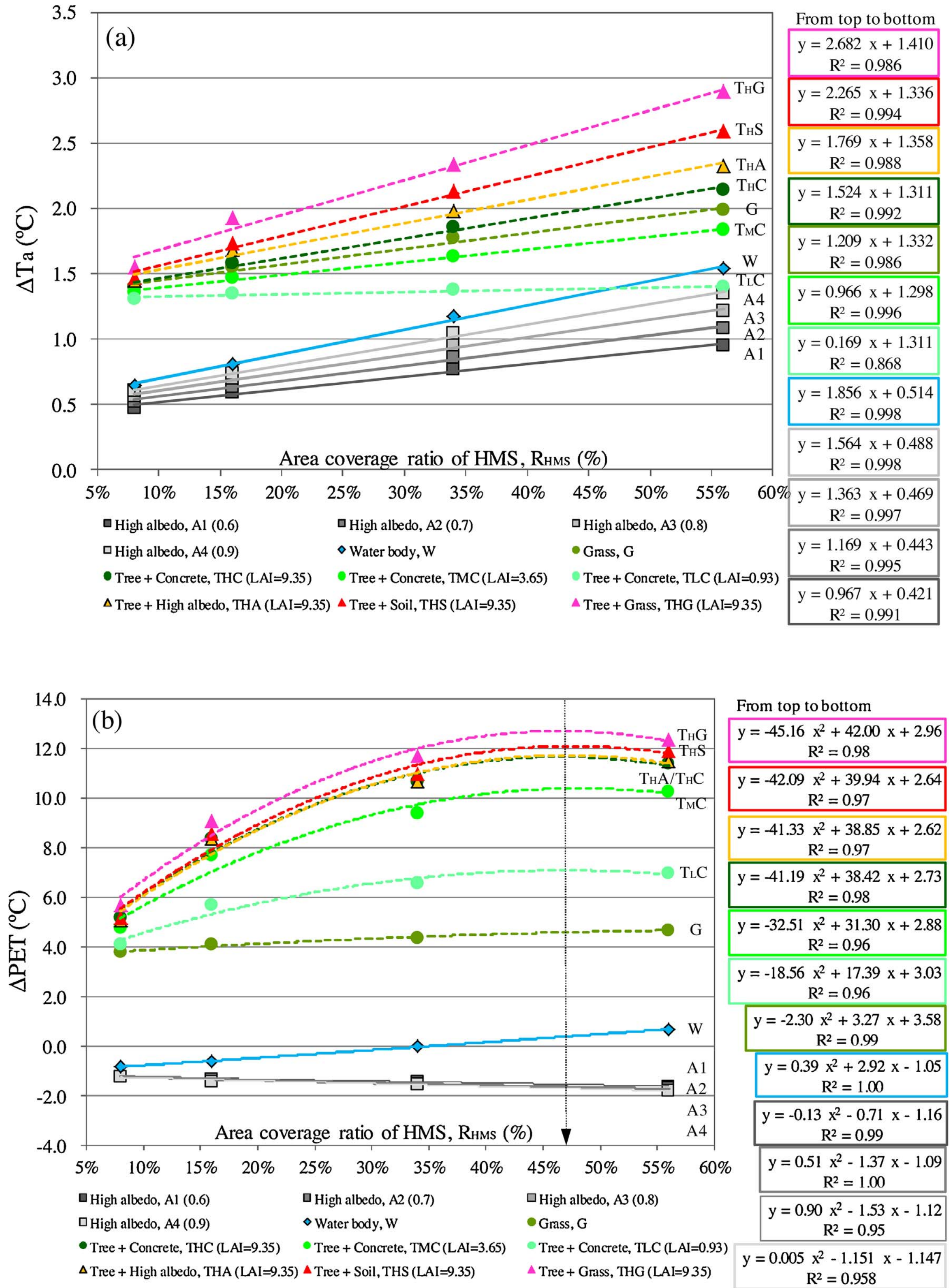

Fig. 7. (a) Characterization Chart A: ΔT_a (°C) against R_{HMS} of different HMS, (b) Characterization Chart B: ΔPET (°C) against R_{HMS} of different HMS.

Hybrid-HMS has good performances in fighting UHI and enhancing human comfort, as reflected from ΔT_a ranges of 1.4–2.2 °C, 1.5–2.3 °C, 1.5–2.6 °C and 1.6–2.9 °C for T_HC, T_HA, T_HS and T_HG, respectively, as well as the corresponding ΔPET ranges of 5.2–11.4 °C, 5.1–11.5 °C, 5.2–11.9 °C and 5.7–12.4 °C. Although Green-HMS is also effective as found from both positive ranges of ΔT_a and ΔPET, Hybrid-HMS could have better and better ΔT_a and ΔPET if the concrete surface was changed to the high albedo pavement, the soil and even the grass.

3.3.2. Generation of characterization charts of heat mitigation strategies

As ΔT_a and ΔPET are effective to quantify the heat mitigation potentials of combating heat island and improving thermal comfort respectively, it would be useful to characterize the performances of Green-HMS, Grey-HMS, Blue-HMS and Hybrid-HMS in different R_{HMS}

graphically. Based on Table 3, two charts can be established: Characterization Chart A for ΔT_a against R_{HMS} as shown in Fig. 7(a), while Characterization Chart B for ΔPET against R_{HMS} in Fig. 7(b).

In Characterization Chart A, a strong linear relationship is observed between ΔT_a and R_{HMS} for each case of HMS, as found from the regression analysis shown on the right hand side of Fig. 7(a). Apparently higher R_{MHS} can have larger ΔT_a. From this chart, Hybrid-HMS demonstrates the greatest heat mitigation potential irrespective of the coverage ratio, followed by Green-HMS, Blue-HMS and Grey-HMS. In each category of landscape design, the effect of the associated design parameter is also presented. For Hybrid-HMS, the order of enhancement of the underneath ground surface, from the most to the least, is T_HG with grass, T_HS with soil, T_HA with high albedo, and T_HC with concrete. For Green-HMS, LAI is another essential design parameter, resulting T_HC the best, T_MC the second and T_LC the last. This demonstrates the landscape design using trees with high LAI is preferable. For Grey-HMS, the albedo value becomes the related design parameter, it is found the bigger, the better. From Chart A, it is observed that water body would outweigh the heat mitigation potential of low-canopy-density trees in case R_{HMS} higher than 47%.

In Characterization Chart B, a second-order polynomial relationship is strongly associated between ΔPET and R_{HMS} for each HMS, as shown from the regression analysis in Fig. 7(b). For consistency and direct comparison, the relationship for the cases without trees is also presented in polynomial. (Actually R^2 of linear relationship for such cases is not better than that of polynomial.) In terms of ΔPET, the ranking of heat mitigation potential of different HMSs is generally the same as ΔT_a. For any case involving trees (T_HG, T_HS, T_HA, T_HC, T_MC and T_LC), ΔPET would have a peak at 47% R_{HMS}, as indicated by a vertical arrow in Fig. 7(b). This can be explained by the complex cooling mechanism of trees. In principle, the denser the tree canopy, the better the shading effect hence better reduction of T_{mrt}, which would enhance the effect of thermal comfort. However, according to Salata, Golasi, de Lieto Vollaro, and de Lieto Vollaro (2015), too dense of tree canopy would obstruct wind speed and intensify relative humidity, causing adverse effect on human comfort. As a result, it can be identified that the best heat mitigation potential with ΔPET happens at R_{HMS} of 47% for the cases with trees, and such benefit is retarded afterwards in Chart B. On the other hand, ΔPET of the cases of G and W are gradually increased with R_{HMS}, but Blue-HMS is only effective when R_{HMS} was greater than 34%. As identified before, Grey-HMS, has negative effect on thermal comfort, no matter what the albedo value is.

3.4. Design insights and recommendations

By using ΔT_a and ΔPET, this study has evaluated the heat mitigation potentials of various landscape designs, including Hybrid-HMS, Green-HMS, Blue-HMS and Grey-HMS, for urban outdoor open space. Generally, these HMSs can provide both positive influences on fighting heat island and improving thermal comfort, except Grey-HMS and certain situation of Blue-HMS. Therefore, it is not enough to enhance the cooling benefit by the common approach of T_a reduction, but also necessary to account for the sociocultural usage through *PET*, which encompasses the integral effect of T_a, *RH*, T_{mrt}, *V*, human clothing and activity. Although the reduced ambient air temperature would help reduce the cooling load of buildings adjacent to the open space, a holistic concern should be given to thermal comfort of the pedestrians outdoors.

Through the two characterization charts established in this study, ΔT_a and ΔPET at any R_{HMS} can be found for a certain landscape design for the urban open space. The heat mitigation potentials of fighting heat island and improving thermal comfort can therefore be quantified. It should be noted that R_{HMS} between 8% and 56% is already the feasible range based on the target assessment area defined in Section 2 for the typical urban morphology, extrapolation of the two charts out of such range is not meaningful. From the family curves of landscape designs in the characterization charts, it helps cover the associated design parameters governing cooling benefit of singular and hybrid HMSs. It is expected that the two charts would be helpful for the design practitioners to understand the extent of various feasible strategies and incorporate them into the urban design accordingly.

4. Conclusions

The cooling potentials of hybrid and singular HMSs, including Hybrid-HMS, Green-HMS, Blue-HMS and Grey-HMS have been quantified in both the aspects of combating heat island and alleviating human heat stress. Findings show that evaluating the heat mitigation potential only in T_a is not sufficient for the urban open space design. Heat stress mitigation from the human biometeorological perspective should also be included. As such, characterization charts of different landscape design are established in terms of both ΔT_a and ΔPET. Such heat mitigation potentials of various HMSs are associated to R_{HMS}, as well as the corresponding design parameters of particular HMS. Characterization Chart A indicates ΔT_a is increased linearly with R_{HMS} in various HMSs. Characterization Chart B depicts clear relationship between ΔPET and R_{HMS}, but in a polynomial instead of linear way. In general, larger R_{MHS} would lead to both higher ΔT_a and ΔPET, except Grey-HMS. Hybrid-HMS exhibits the greatest heat mitigation potentials, followed by Green-HMS, Blue-HMS and Grey-HMS. In fact, Hybrid-HMS has further cooling potentials in decreasing T_a and *PET* compared to those singular landscape designs.

From this study, the essential parameters of landscape design can be consolidated for various strategies as follows:

- Hybrid-HMS: R_{HMS} and ground surface material underneath tree canopy;
- Green-HMS: R_{HMS}, vegetation type and LAI;
- Blue-HMS: $R_{HMS} > 34\%$; and
- Grey-HMS: R_{HMS} and albedo value (for T_a reduction only).

Although, typical urban morphology is used in the current study, it is expected that characterization of various HMSs would help their implementation in urban planning and design practice, so that UHI effect can be moderated in hot and humid climate.

This study primarily focuses on summer daytime heat mitigation. Nevertheless, the effect of urban design on nighttime outdoor thermal environment is an interesting area for future work. Since effective landscape design for daytime cooling may not be beneficial at night due to the heat storage effect of urban fabric. In a diurnal cycle, the heat accumulated is hard to dissipate at night, which would exert a negative influence on daytime heat mitigation of the next day. Hence, future research will help develop a more complete sustainable urban design by incorporating considerations on both daytime and nighttime situations.

Acknowledgement

This work described in this paper is fully supported by a grant from the Research Grants Council of the Hong Kong Special Administrative Region, China (Project No. CityU 123812).

References

ASCE (2004). *Task committee on outdoor human comfort. Outdoor human comfort and its assessment: State of the art.* Virgina: American Society of Civil Engineers.

Ali-Toudert, F. (2005). *Dependence of outdoor thermal comfort on street design in hot and dry climate. Ph.D. thesis.* Freiburg: Freiburg University.

Cui, L., & Shi, J. (2012). Urbanization and its environmental effects in Shanghai, China. *Urban Climate*, *2*, 1–15.

Great Britain. Department of the Environment, Transport and the Regions, Rogers, R.G (1999). *Towards an urban renaissance: Final report of the Urban Task Force*London: Spon.

Jackson, J. B. (1985). Vernacular space. *Texas Architects*, *35*(2), 58–61.

Ng, E., & Cheng, V. (2012). Urban human thermal comfort in hot and humid Hong Kong.

Energy and Buildings, *55*, 51–65.
Ng, E., Chen, L., Wang, Y., & Yuan, C. (2012). A study of the cooling effects of greening in a high-density city: An experience from Hong Kong. *Building and Environment*, *47*, 256–271.
Oke, T. R. (1982). The energetic basis of the urban heat island. *Quarterly Journal of the Royal Meteorological Society*, *108*, 1–24.
Salata, F., Golasi, I., de Lieto Vollaro, A., & de Lieto Vollaro, R. (2015). How high albedo and traditional buildings' materials and vegetation affect the quality of urban microclimate. A case study. *Energy and Buildings*, *99*, 32–49.
Santamouris, M. (2007). Heat island research in Europe: The state of the art. *Advances in Building Energy Research*, *1*(1), 123–150.
Stathopoulos, T. (2006). Pedestrian level winds and outdoor human comfort. *Journal of Wind Engineering and Industrial Aerodynamics*, *94*, 769–780.
Yuminoa, S., Uchidaa, T., Sasaki, K., Kobayashi, H., & Mochidaa, A. (2015). Total assessment for various environmentally conscious techniques from three perspectives: Mitigation of global warming, mitigation of UHIs, and adaptation to urban warming. *Sustainable Cities and Society*, *19*, 236–249.